DOI 10.1007/s11041-022-00795-w
Metal Science and Heat Treatment, Vol. 64, Nos. 5 – 6, September, 2022 (Russian Original Nos. 5 – 6, May – June, 2022)

ALUMINUM AND ITS ALLOYS

UDC 669.715:691.771:669.017.16:621.785.4

STRUCTURE AND PROPERTIES OF Al – Li ALLOY AFTER DIFFERENT ARTIFICIAL AGEING REGIMES AND PRELIMINARY TENSILE DEFORMATION

Peng Zhang[1] and Ming-He Chen[1]

Translated from *Metallovedenie i Termicheskaya Obrabotka Metallov*, No. 5, pp. 10 – 15, May, 2022.

Original article submitted July 20, 2021.

The effect of preliminary 3% tension and artificial ageing regimes on the structure and properties of Al – Li alloy 2A93-T3 sheet is studied. Tensile tests and EBSD analysis of the alloy are conducted. Fracture surfaces are analyzed, and chemical element distribution within the structure is determined. It is established that preliminary tension facilitates failure of coarse T2 and R phases within the structure and formation of fine hardening δ′-phase, a large number of low-angle boundaries and a new S-texture, which increase alloy strength after ageing. A more effective two-stage artificial ageing regime is proposed.

Keywords: aluminum alloy 2A97, preliminary tension, artificial ageing, microstructure, texture.

INTRODUCTION

Al – Li alloys are considered to be very light structural materials [1 – 4]. They have low density, high strength, wear resistance, failure resistance, fatigue crack resistance, and stress corrosion cracking resistance [5, 6], due to which they are most promising for application in the aviation and aerospace industries, including for replacement of traditional high-strength aluminum alloys of the 2000 and 7000 series [6 – 8]. Alloys of a second generation of the Al – Li system such as 2090, 2091, 8090, and 8091 have clearly expressed anisotropy and therefore alloys of a third generation are being developed with good failure resistance [9, 10].

Alloy 2A97 of the Al – Cu – Li system developed within China is related to a third generation of aluminum castable alloys [6]. The alloy is highly alloyed and given heat treatment. After ageing alloy 2A97 it has good strength, failure resistance, corrosion resistance, and also good weldability. It is proposed that alloy 2A97 will be used successfully for preparing aerospace structural elements such as beam structures of an aircraft fuselage body, stringers, panels, lower wall of a wing panel, and fuel tanks [11].

Several publications are well known devoted to studying the properties of alloys 2A97. In [6] evolution of the microstructure and the main mechanism of the three superplastic deformation stages have been studied, and also the mechanism for alloy failure during rolling at 290°C with an initial deformation rate of 3×10^{-3} sec^{-1}. The authors of [12] have studied an elastic aftereffect and strength in tension for alloy in the aged condition and evaluated the effect of various factors on these properties. Tests have been performed in [11] for fatigue at room temperature with the aim of explaining the fatigue crack formation mechanism and also studying the initial stages of alloy 2A97 ageing. Research in [13] was conducted for alloy tensile testing after preliminary deformation in tension with a degree of 3 – 6%. It has been established that preliminary deformation facilitates an increase in ultimate strength and some reduction in relative elongation, and in this case within the alloy structure there is formation of S? and T1 inclusions. Phases have been studied in [14] precipitated during alloy ageing and mechanical properties have been determined after ternary ageing including regression and repeated ageing. It has been demonstrated that this

[1] College of Mechanical & Electrical Engineering, Nanjing University of Aeronautics and Astronautics, Nanjing, Jiangsu, 210016, China (e-mail: 749898443@qq.com).

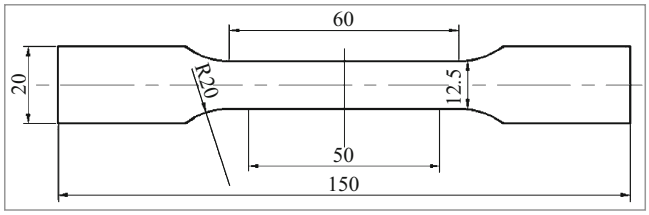

Fig. 1. Alloy 2A97-T3 tensile test specimen.

treatment regime makes it possible to achieve maximum strength properties corresponding to the level of alloy properties after single stage ageing T6 at 165°C. In [15 – 19] the efficiency of friction welding with mixing and laser welding have been studied, and their effect on alloy 2A97 structure has been studied. Also the effect of structure and nature of precipitated secondary phase on alloy corrosion resistance have been studied [20, 21]. However, in spite of a significant amount of research ally 2A97 [22, 27] specific practical recommendations for industrial production providing the properties required, high quality and component dimensional precision, have not yet been made.

The aim of this work is analysis of artificial ageing for alloy 2A07-T3 after quenching and also a study of the effect of preliminary deformation in a quenched condition on alloy structure and properties after ageing by different regimes.

METHODS OF STUDY

For this study sheet 1.5 mm thick of alloy 2A07-T3 produced by the aircraft industry company Xian Aircraft Industry (Group) Co. Ltd. Specimens used in the form of a "dog bone," in accordance with the standard GB/T228.1-2010, were prepared in an electro-erosion cutting mill in the rolling direction (Fig. 1). Tensile testing was performed in a WDW-20E at room temperature and with a constant deformation rate 0.01 sec^{-1} with recording of the stress–strain curve.

The original specimens were subjected to treatment for a solid solution at 520°C for 90 min and then water quenched at room temperature. After this some specimens were deformed in tension to a degree of 3%. The rest of the specimens in this time were within a freezing chamber. Preliminary deformed, and also quenched (but not deformed) specimens were subjected simultaneously to artificial ageing by regimes (*1*) 165°C, 60 h; (*2*) 200°C, 15 h + 165°C, 24 h; (*3*) 200°C, 6 h + 165°C, 6 h. Then all specimens were tensile tested at room temperature.

Specimens for EBSD analysis were prepared by electric spark cutting close to a failure area. Specimen surface was ground with emery paper 1000# and 2000#, and then electropolished in 10% perchloric acid solution and 90% ethanol. Liquid nitrogen was used for cooling the electrolytic polishing liquid. Electropolishing parameters: 20 V; 0.9 – 1.0 A; 15 sec. EBSD analysis was performed in a ZEISS ULTRA 55 scanning electron microscope. A crack was studied using a JSM-6360 scanning electron microscope. Chemical element distribution within the alloy structure was evaluated in a Genesis 2000XM60S energy dispersion spectrometer.

RESULTS AND DISCUSSION

A scanning pitch of 4 μm was established for studying small grains by the EBSD method. EBSD analysis results were processed by means of Channel 5 software making it possible to measure grain misorientation angle and to construct orientation maps by a diffraction backscattered electron method (DOE or EBSD). Grain boundaries with misorientation angles < 10° were considered to be low-angle and with > 10°C they were large angle (green and dark lines in Fig. 2*a* respectively). Analysis of data in Fig. 2*a* showed that in the original sheet material large angle grain boundaries predominate; only a small number of low angle boundaries were observed. In this case according to the orientation map initial orientations ⟨011⟩ and ⟨111⟩ are parallel to the rolling direction (Fig. 2*b*).

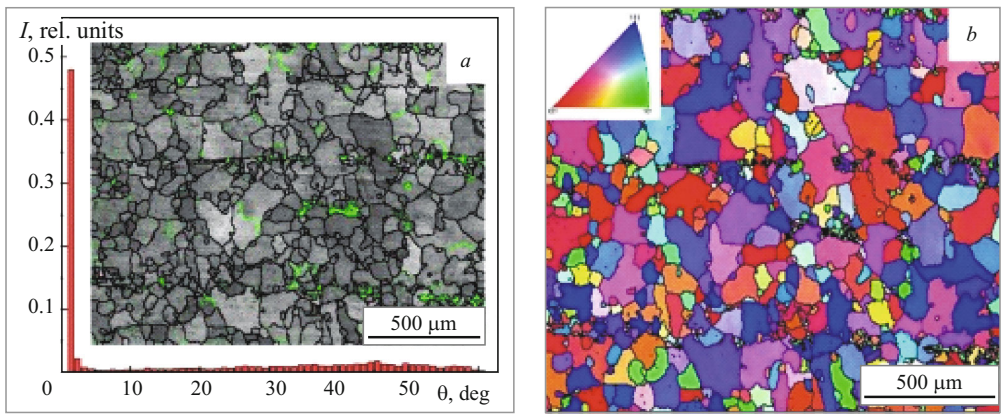

Fig. 2. Grain boundary misorientation (*a*) and orientation (*b*) maps obtained with EBSD of alloy 2A97-T3 sheet in the as-supplied condition: *I* is pulse frequency; θ is misorientation angle.

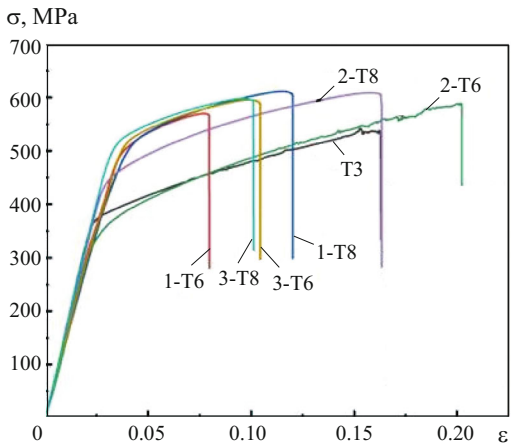

Fig. 3. Stress-strain curves in static tension for alloy 2A97 after various heat treatment; T3 is the as-supplied condition; 1-T6, 2-T6, and 3-T6 are quenching and artificial ageing by regimes *1*, *2*, and *3* respectively; 1-T8, 2-T8, and 3-T8 are quenching, deformation with a degree of 3% and ageing by regimes *1*, *2*, and *3* respectively.

Normally heat treatment of alloy 2A97-T3 consists of high-temperature exposure with subsequent quenching and two-stage artificial ageing.

In the present work alloy 2A97 was heat treated including processing for a solid solution at 520°C, 90 min with subsequent water quenching and single-stage (regime *1*) and two-stage (regimes *2* and *3*) artificial ageing. After heat treatment specimens were studied in static tension at room temperature.

Stress-strain curves obtained are shown in Fig. 3 for alloy 2A97 specimens after various treatment regimes. It is seen that the preliminary tension facilitates an increase in yield and ultimate strength after artificial ageing. Considering the level of mechanical properties achieved and economic indices of the process it was established that the most effective is regime *3* for artificial ageing: 200°C, 6 h + 165°C, 6 h.

The structure is shown in Fig. 4 for alloy 2A97 tensile specimens tested after quenching and artificial ageing by regime *3* with preliminary deformation (ε = 3%) and without it. EBSD analysis close to a specimen failure section showed that the amount of low-angle grain boundaries within the alloy structure increased significantly (especially with use of preliminary tension) compared with the original, i.e., in the as-supplied condition (compare Figs. 2 and 4). These boundaries consist of single dislocations. Consequently, preliminary plastic deformation leads to multiplication and correspondingly an increase in dislocation density during subsequent ageing that facilitates alloy strengthening.

A study of alloy phase composition by the EBSD analysis method showed that in the original condition relatively coarse and nonuniform distribution of phases T2 (Al_6Li_3Cu) and R (Al_5Li_3Cu) (Fig. 5) is present within the structure. Preliminary deformation before artificial ageing facilitates not only a significant increase in dislocation density within the matrix solid solution, but also formation during ageing of a considerable amount of δ′ (Al_3Li) phase inclusions distributed uniformly within the structure (Fig. 6). Therefore, preliminary deformation leads to a change in the type and nature of secondary phase precipitation within the alloy structure during ageing, which also as with an increase in dislocation density increases the alloy set of mechanical properties.

Alloy 2A97 texture in various conditions was evaluated by means orientation distribution function (ODF) and EBSD analysis.

Analysis of the alloy ODF diagram shows the following (Fig. 7).

1. Very strong Euler angle of the alloy structure in the original condition, i.e., 4°, 38°, 45°, orientation {112}[$\bar{1}$10], orientation density $f(g) = 11.1$.

2. After quenching and artificial ageing (3T6) the original texture {112}[$\bar{1}\bar{1}$0] is expressed more weakly and the alloy start to form a new texture.

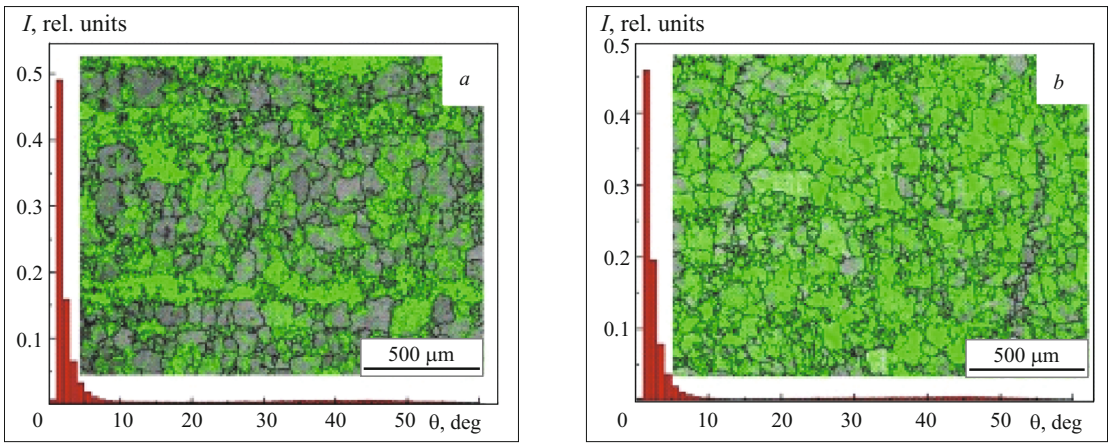

Fig. 4. Grain boundary misorientation maps for alloy 2A97 after heat treatment by regime 3-T6 without prior deformation (*a*) and 3-T8 with preliminary (3%) tensile deformation (*b*): *I* is pulse frequency; θ is misorientation angle.

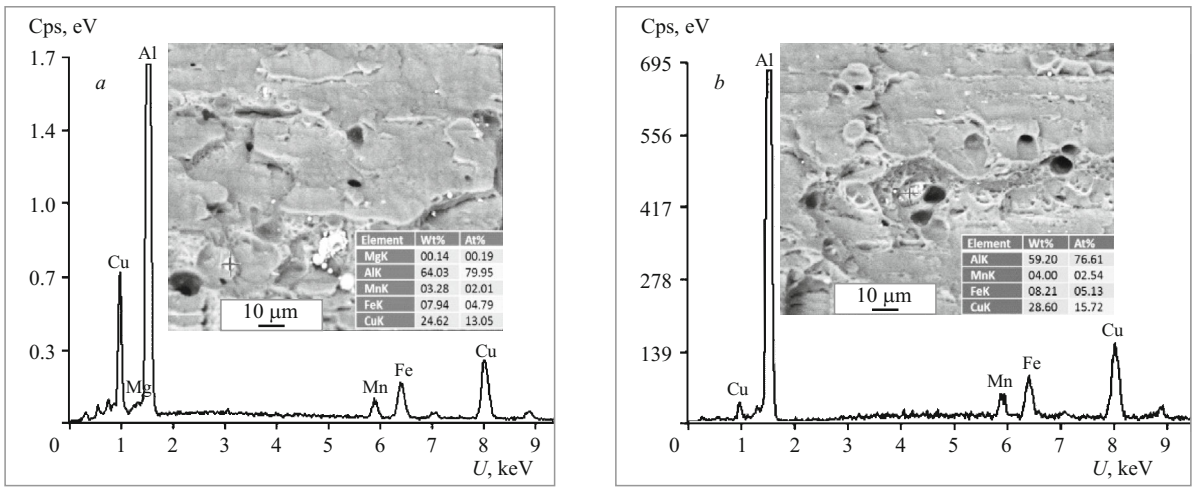

Fig. 5. Inclusions of phases T2 (*a*) and R (*b*) within alloy 2A97-T3 structure in the as-supplied condition and phase analysis results: Wt and At are weight and atomic fractions of elements, %.

3. After heat treatment without preliminary deformation (regime 3-T6) and tensile testing the strongest Euler angles of the alloy texture are 53°, 88°, 45°, orientation {112}[$\bar{1}$12], orientation density $f(g) = 4.65$, which is significantly weaker than in the as-supplied condition.

4. After heat treatment with preliminary deformation (regime 3-T8) and tensile testing a new S-texture forms within the alloy, Euler angles are very strong that equal 2°, 14°, and 45°, orientation {112}[$\bar{1}$10], density $f(g) = 4.08$.

Analysis and comparison of alloy texture shows that after heat treatment, including quenching and artificial ageing by regime *3*, the texture changes compared with the original. After the same heat treatment, but with preliminary ($\varepsilon = 3\%$) deformation before ageing, there is formation of a new S-type texture within the alloy.

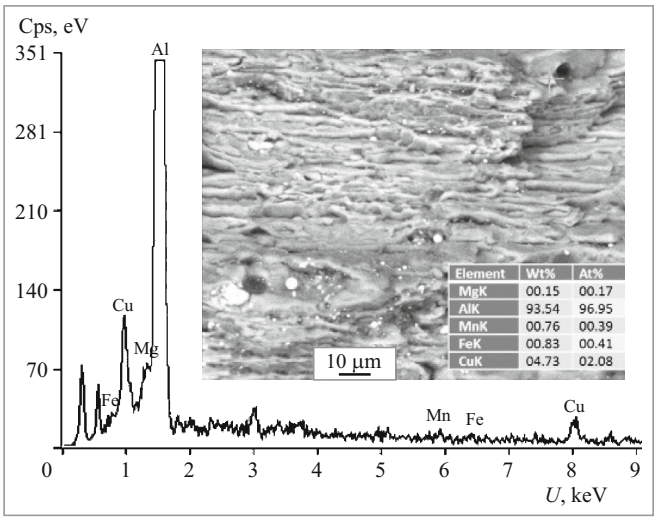

Fig. 6. Inclusions of δ′-phase within alloy 2A97 structure after heat treatment by regime 3-T8 and phase analysis results.

As a result of preliminary deformation within the alloy structure there is an increase in dislocation density for the matrix that may lead to a change in texture type and nature of secondary phase distribution separated during ageing. As a result of this alloy 2A97 mechanical properties are improved. It is typical that the orientation density after this alloy treatment decreases significantly compared with the original. Reasons for this, and also formation of a new structure are the alloy heat treatment and plastic deformation.

CONCLUSIONS

1. The structure and properties of alloy 2A97-T3 of the Al – Cu – Li system have been studied after heat treatment including quenching, preliminary tensile deformation ($\varepsilon = 3\%$) and artificial ageing by regimes (*1*) 165°C, 60 h; (*2*) 200°C, 15 h + 165°C, 24 h; (*3*) 200°C, 6 h + 165°C, 6 h.

2. All of the artificial ageing regimes studied facilitate a significant increase in alloy yield point and strength. The most effective is regime *3*.

3. Use of preliminary plastic deformation before alloy ageing facilitates a significant increase in dislocation density, an increase in the amount of low-angle grain boundaries within the structure, and also formation of a new S-type texture and a reduction in orientation density that is a reason for an increase in alloy strength properties with some reduction in ductility.

4. In the as-supplied condition within the structure of alloy 2A97-T3 sheet coarse inclusions of phase T2 and R are present. After treatment, including preliminary tension by 3%, quenching, and ageing within the alloy structure there is formation of fine uniformly distributed inclusions of secondary δ′-phase (Al_3Li) that facilitates an increase in alloy operating properties.

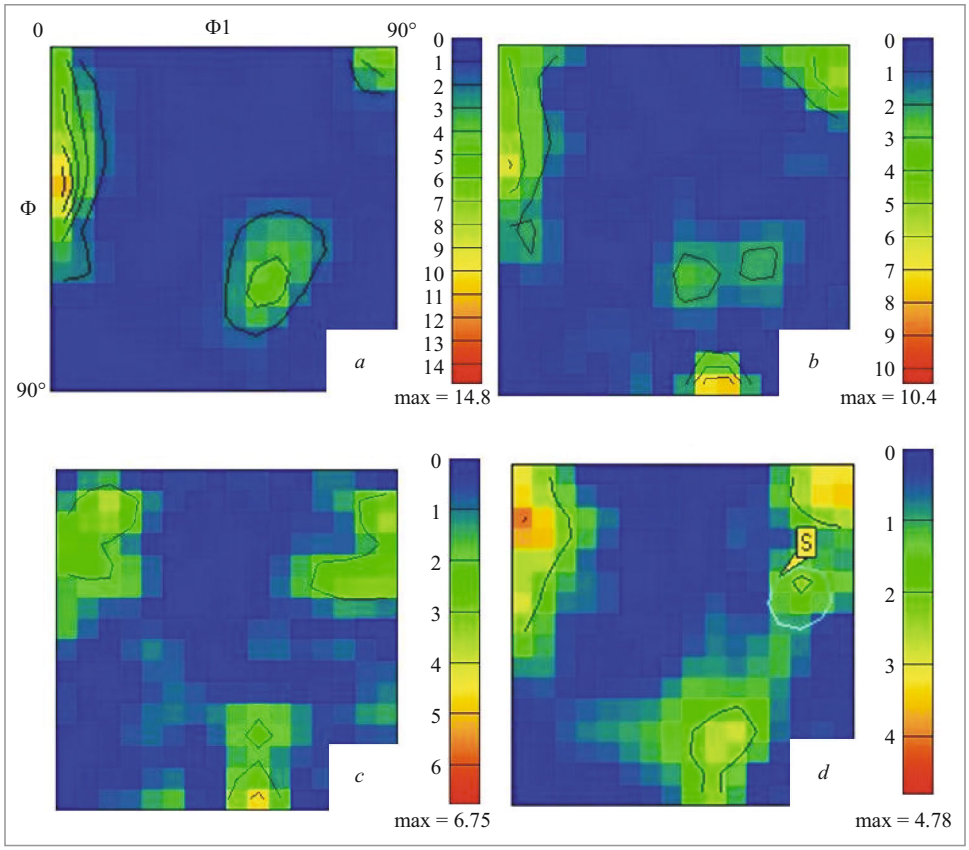

Fig. 7. Alloy 2A97 texture (orientation distribution function (ODF) with $\psi_2 = 45°$) in the as-supplied condition T3 (*a*), after heat treatment by regime 3-T6 (*b*), after heat treatment by regime 3-T6 (*c*) and 3-T8 (*d*) and static tensile testing.

This research was carried out with funding from the National Natural Science Funds of China (Grant No. 51175252). The authors would like to acknowledge assistance of these programs for the financial support. And the EBSD were provided technical support by "Ceshigo Research Service" www.ceshigo.com.

REFERENCES

1. J. R. J. X. Raj and B. P. Shanmugavel, "Thermal stability of ultrafine grained AA8090 Al – Li alloy processed by repetitive corrugation and straightening," *J. Mater. Res. Technol*., **8**, No. 3, 3251 – 3260 (2019).
2. F. Liu, Z. Liu, M. Liu, et al., "Analysis of empirical relation between microstructure, texture evolution and fatigue properties of an Al – Cu – Li alloy during different pre-deformation processes," *Mater. Sci. Eng. A*, **726**, 309 – 319 (2018).
3. Z. Jin, L. Zhide, X. Fushun, et al., "Regulating effect of pre-stretching degree on the creep aging process of Al – Cu – Li alloy," *Mater. Sci. Eng. A*, **763**, 138157 (2019).
4. L. Hu, L. Zhan, Z. Liu, et al., "The effects of pre-deformation on the creep aging behavior and mechanical properties of Al – Li – S4 alloys," *Mater. Sci. Eng. A*, **703**, 496 – 502 (2017).
5. Y. Lin, C. Lu, C. Wei, et al., "Effect of aging treatment on microstructures, tensile properties and intergranular corrosion behavior of Al – Cu – Li alloy," *Mater. Charact*., **141**, 163 – 168 (2018).
6. L. Jia, R. Xueping, H. Hongliang, and Z. Yanling, "Microstructural evolution and superplastic deformation mechanisms of as-rolled 2A97 alloy at low-temperature," *Mater. Sci. Eng. A*, **759**, 19 – 29 (2019).
7. Z. Liwei, G. Wenli, G. Zhaohui, et al., "Hot deformation characterization of as-homogenized Al – Cu – Li X2A66 alloy through processing maps and microstructural evolution," *J. Mater. Sci. Technol*., **35**, 2409 – 2421 (2019).
8. A. Abd El-Aty, Y. Xu, X. Guo, et al., "Strengthening mechanisms, deformation behavior, and anisotropic mechanical properties of Al – Li alloys: A review," *J. Adv. Res*., **10**, 49 – 67 (2018).
9. T. Dursun and C. Soutis, "Recent developments in advanced aircraft aluminium alloys," *Mater. Des*., **56**, 862 – 871 (2014).
10. W. Fan, B. P. Kashyap, and M. C. Chaturvedi, "Anisotropy in flow and microstructural evolution during superplastic deformation of a layered-microstructured AA8090 Al – Li alloy," *Mater. Sci. Eng. A*, **349**(1 – 2), 166 – 182 (2003).
11. J. Zhong, S. Zhong, Z. Q. Zheng, et al., "Fatigue crack initiation and early propagation behavior of 2A97 Al – Li alloy," *Trans. Nonferrous Met. Soc. Chin*., **24**(2), 303 – 309 (2014).
12. H. Y. Li and X. C. Lu, "Springback and tensile strength of 2A97 aluminum alloy during age forming," *Trans. Nonferrous Met. Soc. Chin*., **25**(4), 1043 – 1049 (2015).

13. C. Gao, Y. Luan, J. C. Yu, et al., "Effect of thermo-mechanical treatment process on microstructure and mechanical properties of 2A97 Al – Li alloy," *Trans. Nonferrous Met. Soc. Chin*., **24**, 2196 – 2202 (2014).
14. Z. S. Yuan, L. U. Zheng, Y. H. Xie, et al., "Effects of RRA treatments on microstructures and properties of a new high-strength aluminum-lithium alloy-2A97," *Chin. J. Aeronautics*, **20**, 187 – 192 (2007).
15. C. Gao, R. Gao, and Y. Ma, "Microstructure and mechanical properties of friction spot welding aluminium – lithium 2A97 alloy," *Mater. Des*., **83**, 719 – 727 (2015).
16. J. Ning, L. J. Zhang, Q. L. Bai, et al., "Comparison of the microstructure and mechanical performance of 2A97 Al – Li alloy joints between autogenous and non-autogenous laser welding," *Mater. Des*., **120**, 144 – 156 (2017).
17. H. Chen, L. Fu, P. Liang, et al., "Defect features, texture and mechanical properties of friction stir welded lap joints of 2A97 Al – Li alloy thin sheets," *Mater. Charact*,. **125**, 160 – 173 (2017).
18. H. Chen, L. Fu, and P. Liang, "Microstructure, texture and mechanical properties of friction stir welded butt joints of 2A97 Al – Li alloy ultra-thin sheets," *J. Alloys Compd*., **692**, 155 – 169 (2017).
19. L. Chen, Y. N. Hu, E. G. He, et al., "Microstructural and failure mechanism of laser welded 2A97 Al – Li alloys via synchrotron 3D tomography," *Int. J. Lightweight Mater. Manufac*., **1**, 169 – 178 (2018).
20. X. Zhang, X. Zhou, T. Hashimoto, et al., "The influence of grain structure on the corrosion behaviour of 2A97-T3 Al – Cu – Li alloy," *Corros. Sci*., **116**, 14 – 21 (2017).
21. X. Zhang, X. Zhou, T. Hashimoto, et al., "Corrosion behaviour of 2A97-T6 Al – Cu – Li alloy: The influence of non-uniform precipitation," *Corros. Sci*., **132**, 1 – 8 (2018).
22. G. Chen, M. Chen, N. Wang, et al., "Hot forming process with synchronous cooling for AA2024 aluminum alloy and its application," *Int. J. Adv. Manufac. Technol*., **86**, 133 – 139 (2016).
23. X. Fan, Z. He, K. Zheng, et al., "Strengthening behavior of Al – Cu – Mg alloy sheet in hot forming – quenching integrated process with cold – hot dies," *Mater. Des*., **83**, 557 – 565 (2015).
24. X. Fan, Z. He, S. Yuan, et al., "Experimental investigation on hot forming – quenching integrated process of 6A02 aluminum alloy sheet," *Mater. Sci. Eng. A*., **573**, 154 – 160 (2013).
25. H. Li, X. Guo, W. Wang, et al., "Forming performance of an as-quenched novel aluminum-lithium alloy," *Int. J. Adv. Manufac. Technol*., **78**, 659 – 666 (2015).
26. M. L. Wang, P. P. Jin, J. H. Wang, et al., "Hot deformation behavior of as-quenched 7005 aluminum alloy," *Trans. Nonferrous Met. Soc. Chin*., **24**(9), 2796 – 2804 (2014).
27. X. W. Yang, Z. H. Lai, J. C. Zhu, et al., "Hot compressive deformation behavior of the as-quenched A357 aluminum alloy," *Mater. Sci. Eng. B*, **177**, 1721 – 1725 (2012).